



Rising Stars: *In vivo* Monitoring of Neurochemical Dynamics by Genetically Encoded Neuromodulator Sensors [☆]

Shengwei Fu ^{1,2,3}, and Yulong Li ^{1,2,3,4,*}

1 - Peking-Tsinghua Center for Life Sciences, Academy for Advanced Interdisciplinary Studies, Peking University, Beijing 100871, China

2 - PKU-IDG/McGovern Institute for Brain Research, New Cornerstone Science Laboratory, Beijing 100871, China

3 - State Key Laboratory of Membrane Biology, Peking University School of Life Sciences, Beijing 100871, China

4 - National Biomedical Imaging Center, Peking University, Beijing 100871, China

Correspondence to Yulong Li: Peking-Tsinghua Center for Life Sciences, Academy for Advanced Interdisciplinary Studies, Peking University, Beijing 100871, China. yulongli@pku.edu.cn (Y. Li)

<https://doi.org/10.1016/j.jmb.2026.169669>

Edited by Da Jia

Abstract

Dr. Yulong Li received his undergraduate education in biophysics and physiology at Peking University, and subsequently completed his Ph.D. training under the mentorship of Dr. George J. Augustine at Duke University, where he investigated fundamental mechanisms of synaptic transmission. He then pursued postdoctoral research in the laboratory of Dr. Richard W. Tsien at Stanford University, where he began developing genetically encoded indicators for applications in neuroscience. Since 2012, Dr. Yulong Li established his lab at Peking University. His research has been at the forefront of developing the genetically encoded fluorescent sensors for neurotransmitters and neuromodulators, which have emerged as powerful tools for real-time monitoring of the dynamic changes of these molecules with high sensitivity, selectivity, spatiotemporal resolution, and minimal invasiveness *in vivo*. This article provides a comprehensive overview of the design strategies and key progress in this rapid evolving field, emphasizing how these tools have transformed the study of neuromodulation.

© 2026 Elsevier Ltd. All rights are reserved, including those for text and data mining, AI training, and similar technologies.

Introduction

The human brain consists of billions of neurons interconnected by chemical synapses, where communication is mediated by the release of neurotransmitters and neuromodulators [1]. Classic neurotransmitters, such as glutamate and γ -aminobutyric acid (GABA), typically mediate rapid point-to-point synaptic transmission by activating ionotropic receptors, sometimes also acting through metabotropic G protein-coupled receptors (GPCRs)

[2]. On the other hand, neuromodulators, such as monoamines, neuropeptides, and neurolipids, exert their effects mainly through GPCRs to trigger downstream signaling cascades in a relatively slower and long-range way through diffusion [3,4]. Neuromodulators play crucial roles in regulating neurotransmission in specific neural circuits, thereby influencing diverse physiological processes, such as cognition, motor control, mood, homeostasis, and learning and memory. Consequently, disruptions in neuromodulatory signaling have been associated with many psychiatric and neurological disorders, including depression [5,6], schizophrenia [7,8], Parkinson's disease [9,10], and Alzheimer's disease [11,12].

[☆] This article is part of a special issue entitled: 'Pioneers in Molecular Biology (China)' published in Journal of Molecular Biology.

Given their fundamental roles in brain function, the ability to monitor neuromodulator dynamics with high precision is crucial for understanding their regulatory mechanisms under both physiological and pathological conditions. However, traditional detection methods, including microdialysis [13–15], electrochemical [16–18], and electrophysiological methods [19], are limited by their spatiotemporal resolution and invasiveness, making it difficult to faithfully report the rapid changes of neuromodulators, especially in behaving animals. Over the past few years, the development of genetically encoded fluorescent sensors for neuromodulators has provided a transformative solution to these limitations. These sensors offer high spatial and temporal resolution, molecular specificity, and minimal invasiveness, enabling real-time monitoring of neuromodulator dynamics *in vivo* across various model organisms, including fruit flies, zebrafish, and mice. This review summarizes the design principles, recent progress, and applications of these sensors and discusses future directions of sensor development, aimed at enhancing their utility for neuroscience research.

Design principles of neuromodulator fluorescent sensors

Genetically encoded neuromodulator fluorescent sensors typically consist of two key components: a fluorescent reporting module and a ligand recognition module. These sensors function by selectively binding to a target neuromodulator via the ligand recognition module, which induces a conformational change that is transduced to the fluorescent reporting module, thereby generating a detectable fluorescence signal change [20,21]. Compared with the Förster resonance energy transfer (FRET)-based strategy, single-fluorophore sensors typically use circularly permuted fluorescent proteins (cpFPs) as the fluorescent reporting module, thereby offering advantages such as compact size, large dynamic range, and ability to perform multi-color imaging. Depending on the design strategy of the ligand recognition module, neuromodulator sensors are generally categorized into two major categories: those based on periplasmic binding proteins (PBPs) and those based on GPCRs (Table 1).

PBP-based neuromodulator sensors

PBP-based sensors are constructed by fusing bacterial binding proteins to environmentally sensitive cpFPs. PBP domain recognizes and binds to target neuromodulators, undergoing conformational changes upon ligand binding that alter the fluorescence signal of the connected cpFP (Figure 1A) [22]. These PBP-based sensors can be efficiently screened in bacterial systems, allowing for high-throughput optimization. As a result, they often exhibit high brightness and sensi-

tivity, making them suitable for precise monitoring of specific neurochemicals release, such as iGluSnFR series [23–25], iAChSnFR [26], iATPSnFR [27], and iSeroSnFR [28]. Because neuromodulators are typically released into the extracellular space, sensors need to be correctly localized to the plasma membrane of neuronal cells to capture neuromodulatory dynamics. However, achieving efficient membrane targeting and functional expression of PBP-based sensors in mammalian systems has proven challenging. To address this issue, recent efforts have focused on incorporating various membrane-targeting sequences to improve the membrane expression of PBP-based sensors in mammalian cells [28]. In addition, the evolutionary divergence between prokaryotic PBPs and mammalian signaling systems may result in suboptimal ligand affinity and response kinetics, limiting their ability to faithfully report endogenous neuromodulator dynamics [27]. More importantly, there is often no direct bacterial homolog for many mammalian neuromodulators, particularly neuropeptides, making it difficult to develop highly specific sensors. Although emerging machine learning approaches offer the potential to reengineer the ligand-binding pocket of PBPs for improved affinity and selectivity, such modifications may compromise sensor sensitivity or dynamic range, significantly hindering their utility *in vivo* [28].

GPCR-based neuromodulator sensors

GPCRs represent the largest family of membrane proteins and have naturally evolved to function as highly sensitive neuromodulator sensors. They are capable of detecting a wide range of extracellular signaling molecules—including neurotransmitters and neuromodulators—with high sensitivity and specificity, making them ideal candidates to serve as ligand recognition modules in the GPCR-activation based (GRAB) strategy. Furthermore, many neuromodulators act through multiple GPCR receptor subtypes, each exhibiting distinct affinities and response kinetics for ligand binding. For instance, more than ten subtypes of serotonin (5-HT) receptors have been identified in human and mouse, each differing in 5-HT affinities and pharmacological properties [29,30]. In addition, the evolutionary conservation of GPCRs across species offers a diverse set of receptors that can be leveraged for sensor design and optimization.

Inspired by the mechanistic insight into GPCR activation, GPCR-based sensors—such as the GRAB sensors and the Light series sensors—exploit GPCRs that specifically bind neuromodulators and undergo conformational changes, particularly at the cytoplasmic end of the fifth and sixth transmembrane domain (TM5 and TM6) [31–36]. These sensors translate neuromodulator binding into changes in fluorescence intensity by coupling the conformational changes of GPCRs to environmentally sensitive cpFP (Figure 1B). This versatile strategy has enabled the development of a

Table 1 Summary of genetically encoded neuromodulator sensors.

Neuromodulator	Sensor name	Fluorescence	Scaffold protein	Maximum response (%)	EC ₅₀ (μM)		On kinetics (s)	Off kinetics (s)	References
Glu	iGluSnFR	Green	<i>Escherichia coli</i> GltI	400	4		0.015 ^a (τ _{1/2})	0.092 ^a (τ _{1/2})	[23]
Glu	SF-Venus-iGluSnFR. A184V	Green	<i>Escherichia coli</i> GltI	200	2 ^b		NA	NA	[24,25]
Glu	iGluSnFR3 v857	Green	<i>Escherichia coli</i> GltI	1750	8.2 ^b		NA	NA	[25]
Glu	iGluSnFR3 v82	Green	<i>Escherichia coli</i> GltI	750	4.5 ^b		NA	NA	[25]
ACh	iAChSnFR	Green	<i>Thermoanaerobacter</i> sp. X513 OpuBC	1000	2.9		NA ^c	NA ^c	[26]
5-HT	iSeroSnFR	Green	<i>Bacillus subtilis</i> OpuBC	1700	390		0.0005–0.01 (fast phase); 5–18 (slow phase)	NA	[27]
ATP	iATPSnFR1.0	Green	<i>Methanococcus jannaschii</i> GlnK1	100	350		0.3–1.8	1.2–3.2	[28]
ATP	iATPSnFR1.1	Green	<i>Methanococcus jannaschii</i> GlnK1	88	138		0.5–4.8	1.2–3.8	[28]
Neuromodulator	Sensor name	Fluorescence	Scaffold protein	Maximum response (%)	EC ₅₀ (nM)	Specificity fold ^d	On kinetics (s)	Off kinetics (s)	References
DA	DA1m	Green	Human D2R	90	130	13	0.06	0.71	[39]
DA	DA1h	Green	Human D2R	90	10	9.7	0.14	2.52	[39]
DA	rDA1m	Red	Human D2R	150	95	22	0.08	0.77	[42]
DA	rDA1h	Red	Human D2R	100	4	15	0.06	2.15	[42]
DA	DA2m	Green	Human D2R	340	90	15	0.04	1.3	[42]
DA	DA2h	Green	Human D2R	280	7	10	0.05	7.3	[42]
DA	gDA3m	Green	Human D1R	1000	86	80 ^b	0.069	0.56	[49]
DA	gDA3h	Green	Bovine D1R	1240	22	45 ^b	0.048	1.85	[49]
DA	rDA2m	Red	Red fire ant D2R	560	180	60 ^b	0.05	2.24	[49]
DA	rDA2h	Red	Red fire ant D2R	240	9	70	0.05	3.35	[49]
DA	rDA3m	Red	Human D1R	1460	130	20 ^b	0.064	0.61	[49]
DA	rDA3h	Red	Human D1R	1520	20	12	0.06	3.6	[49]
DA	HaloDA1.0 ^e	Far-red	Human D1R	900	150	16	0.04	3.08	[52]
DA	dLight1.1	Green	Human D1R	230	330	60	NA	NA	[40]
DA	dLight1.2	Green	Human D1R	340	770	NA	0.0095 ^f (τ _{1/2})	0.09 ^f (τ _{1/2})	[40]
DA	dLight1.3b	Green	Human D1R	930	1680	NA	NA	NA	[40]
DA	dLight1.4	Green	Human D1R	170	4	NA	NA	NA	[40]
DA	RdLight1	Red	Human D1R	248	859	60	0.014 ^f	0.398 ^f	[43]
NE	NE1m	Green	Human α2AR	230	930	350	0.072	0.68	[41]
NE	NE1h	Green	Human α2AR	130	83	37	0.036	1.89	[41]

(continued on next page)

Table 1 (continued)

Neuromodulator	Sensor name	Fluorescence	Scaffold protein	Maximum response (%)	EC ₅₀ (μM)	On kinetics (s)	Off kinetics (s)	References	
NE	NE2m	Green	Human α2AR	381	380	53	0.12	1.72	[48]
NE	NE2h	Green	Human α2AR	415	190	47	0.09	1.93	[48]
NE	nLightG	Green	Sperm whale α1AR	1083	755	26	0.023	0.194	[47]
NE	nLightR	Red	Sperm whale α1AR	158	654	28	NA	NA	[47]
Neuromodulator	Sensor name	Fluorescence	Scaffold protein	Maximum response (%)	EC ₅₀ (nM)	On kinetics (s)	Off kinetics (s)	References	
5-HT	5-HT1.0	Green	Human 5-HT2CR	250	22	0.2	3.13	[44]	
5-HT	5-HT2m	Green	Mouse 5-HT4R	1400	1100	0.12	0.38	[50]	
5-HT	5-HT2h	Green	Mouse 5-HT4R	600	80	0.1	1.9	[50]	
5-HT	g5-HT3.0	Green	Mouse 5-HT4R	1300	150	0.29	1.66	[50]	
5-HT	r5-HT1.0	Red	Mouse 5-HT4R	330	790	0.05	0.51	[50]	
5-HT	psychLight1	Green	Human 5-HT2AR	79.6	26.3	NA	NA	[45]	
5-HT	psychLight2	Green	Human 5-HT2AR	NA	NA	NA	0.997 (fast); 3.998 (slow) ^f	[45]	
4 5-HT	sDarken	Green	Human 5-HT1AR	-70	127	0.0435	0.323	[86]	
HA	HA1m	Green	Water bear H1R	590	380	0.3	1.4	[46]	
HA	HA1h	Green	Human H4R	370	17	0.6	2.3	[46]	
OA	OA1.0	Green	Drosophila Octβ2R	660	200	0.02	1.4	[51]	
ACh	ACh2.0	Green	Human M3R	90	700	0.28	0.762	[37]	
ACh	ACh3.0	Green	Human M3R	280	2200	0.112 ^g	0.58 ^g	[38]	
ATP	ATP1.0	Green	Human P2Y1R	500	80	0.028	0.283	[54]	
Ado	Ado1.0	Green	Human A2AR	120	60	0.068	16	[53]	
Ado	Ado1.0m	Green	Human A2AR	350	3200	NA	NA	[55]	
UDP	UDP1.0	Green	Chicken P2Y6R	600	91	NA	NA	[56]	
eCB	eCB2.0	Green	Human CB1R	300	200 (AEA); 3100 (2-AG)	1.6	11.2	[57]	
PGD2	PGD2-1.0	Green	Bat DP1R	200	12	NA	NA	[58]	
PGD2	PGD2-1.1	Green	Bat DP1R	340	5.7	NA	NA	[58]	
OT	OT1.0	Green	Bovine OTR	410	3	0.48	NA	[59]	
OT	MTRIA _{OT}	Green	Medaka OTR	735	20.5	1.2	26	[60]	
SST	SST1.0	Green	Human SSTR5	430	69 (SST-14); 13 (SST-28)	0.28	4.5	[61]	
CRF	CRF1.0	Green	Human CRF1R	1200	33	0.4	12	[61]	
CCK	CCK1.0	Green	Human CCKBR	840	2.9 (CCK-4); 4 (CCK-8s)	0.3	18	[61]	
NPY	NPY1.0	Green	Human NPY1R	490	43	0.37	NA	[61]	
NTS	NTS1.0	Green	Human NTSR1	250	6	0.2	14	[61]	

Table 1 (continued)

Neuromodulator	Sensor name	Fluorescence	Scaffold protein	Maximum response (%)	EC ₅₀ (μM)	On kinetics (s)	Off kinetics (s)	References
VIP	VIP1.0	Green	Human VIPR2	360	19	0.91	NA	[61]
OX	Hcrt0.5 (OX0.5)	Green	Human OX2R	1100	210 (orexin-A); 100 (orexin-B)	NA	NA	[64]
OX	OxLight1	Green	Human OX2R	900 (orexin-A); 860 (orexin-B)	75 (orexin-A); 47 (orexin-B)	0.60 (orexin-A); 0.62 (orexin-B)	NA	[66]
sNPF	sNPF1.0	Green	<i>Culex quinquefasciatus</i> sNPF	300	64	0.21 ^h	4.64 ^h	[65]
GLP-1	GLPLight1	Green	Human GLP1R	528	27.6	4.7	NA	[67]
Opioid	κLight1.3	Green	Human κOR	93.6	0.0898 (DynA13)	NA	NA	[69]
Opioid	δLight	Green	Human δOR	246	6.5 (ME)	NA	NA	[69]
Opioid	μLight	Green	Human μOR	55	1680 (β-endorphin)	NA	NA	[69]
N/OAQ	NOPLight	Green	Human NOPR	388	28.65	0.595	29.9	[68]

For consistency, data from HEK cell expression assays are preferentially selected, where reported in the original literature. NA, not available.

^a Determined in cultured neurons upon single field stimulus.

^b Determined in cultured neurons.

^c Stopped-flow kinetic analysis of purified iAChSnFR shows $k_{on} = 0.62 \mu\text{M}^{-1} \text{s}^{-1}$ and $k_{off} = 0.73 \text{s}^{-1}$.

^d For DA sensors, the specificity fold is defined as the ratio of the EC₅₀ value for NE to that for DA; for NE sensors, the specificity fold is defined as the ratio of the EC₅₀ value for DA to that for NE.

^e Labeled with JF646-HTL.

^f Determined in acute brain slices upon a single electrical stimulus.

^g Measured in the presence of 100 μM ACh. $k_{on} = 3.12 \mu\text{M}^{-1} \text{s}^{-1}$ and $k_{off} = 1.72 \text{s}^{-1}$.

^h Measured in the presence of 10 μM sNPF. $k_{on} = 421 \mu\text{M}^{-1} \text{s}^{-1}$.

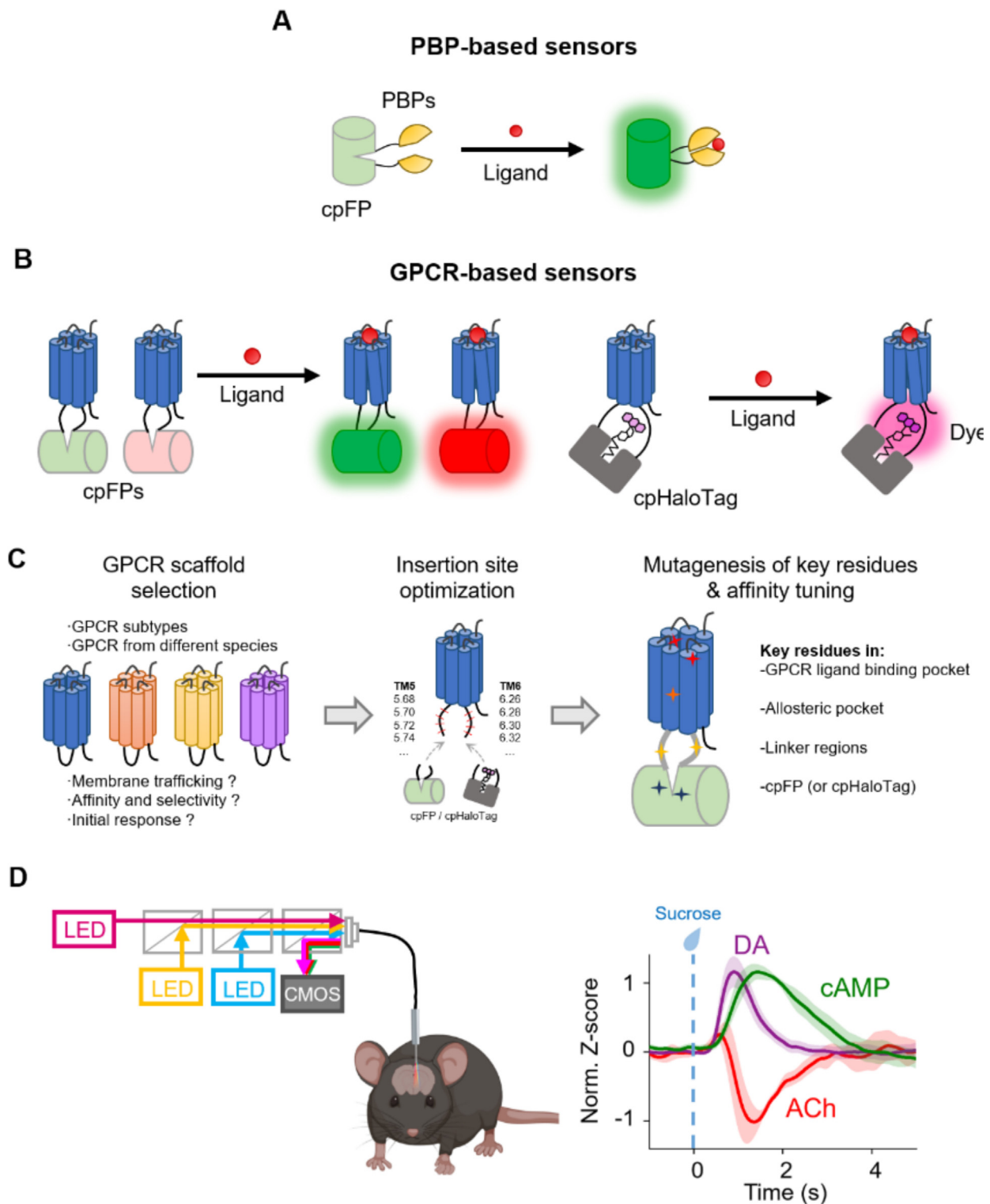


Figure 1. Genetically encoded neuromodulator sensors. (A) Periplasmic binding protein (PBP)-based sensors. (B) G protein-coupled receptor (GPCR)-based sensors, such as GRAB sensors. The fluorescent module can be either circularly permuted fluorescent proteins (cpFPs), or protein tags covalently labeled with chemical dyes which are effective for developing sensors in the far-red and near-infrared spectral ranges. (C) The workflow of GRAB sensor engineering, including GPCR scaffold selection, insertion site optimization, mutagenesis of key residues, and affinity tuning. (D) Simultaneous monitoring of dopamine (DA), acetylcholine (ACh), and cyclic adenosine 5'-monophosphate (cAMP) dynamics *in vivo*. DA, ACh, and cAMP level changes are recorded from HaloDA1.0, rACh1h, and GFlamp2 signals, respectively. Data are replotted from Zheng et al. [52].

wide range of neuromodulator sensors for acetylcholine (ACh) [37,38], monoamine neuromodulators [39–52], purines [53–56], neurolipids [57,58], and neuropeptides [59–69]. The GRAB and Light series sensors are well suited for detecting endogenous neuromodulator release across various physiological and pathological contexts, and they have been successfully applied in primary neurons, acute brain slices, fruit flies, zebrafish, and living mice.

Beyond cpFPs, recent advancements have highlighted the use of circularly permuted self-labeling proteins, such as cpHaloTag, in combination with synthetic chemical dyes as alternative fluorescent domains for chemigenetic biosensors (Figure 1B) [70–72]. The cpHaloTag protein, covalently labeled with environment sensitive rhodamine derivatives via the HaloTag ligand (HTL), enables fluorescence emission spanning from green to near-infrared (500–700 nm), while offering not only higher brightness and improved photostability, but also the potential to attain a higher dynamic range of sensors engineered with cpHaloTag [73].

Upon ligand binding, GPCRs undergo rapid conformational changes, with the most pronounced shifts occurring in the third intracellular loop (ICL3) located between the TM5 and TM6 domains. In the construction of neuromodulator sensors, either cpFPs or cpHaloTag are typically inserted into this region, followed by multiple rounds of optimization. For GRAB sensors, the development and optimization process generally involve four essential steps (Figure 1C): (i) *Screening of GPCR sources and subtypes*: cpFP/cpHaloTag is inserted into the ICL3 of various GPCR subtypes or homologs from different species. Prototype sensors are then evaluated for key properties, including membrane trafficking, dynamic range, ligand affinity, and specificity, to select an optimal receptor scaffold. (ii) *Optimization of cpFP/cpHaloTag insertion sites*: The cpFP/cpHaloTag insertion site is systematically screened in a stepwise manner. Then the ICL3, including the linkers flanking the cpFP/cpHaloTag, is progressively truncated to improve the coupling between ligand-induced conformational changes and fluorescence responses, thereby identifying the optimal insertion position. (iii) *Mutagenesis of key residues*: Saturated mutagenesis is performed on critical residues within the linker regions, cpFP/cpHaloTag, and potentially relevant sites in the GPCR scaffold. This step aims to enhance the signal-to-noise ratio and maximize sensor performance. (iv) *Tuning of the sensor affinity*. To accommodate varying concentrations of neuromodulators across different brain regions and physiological states, additional saturated mutagenesis is carried out in the ligand-binding pocket of the GPCR or other regions influencing ligand interaction, which yields sensor variants

with a range of affinities. Ligand-insensitive mutant versions can also be generated as negative controls.

In the characterization of a series of GRAB sensors, researchers have found that these sensors typically exhibit no detectable coupling to endogenous downstream signal transduction pathways of GPCRs, including G protein-mediated signaling and the β -arrestin pathways [37–39,41,42,44,46,48–52,54,57,59,61,65]. Moreover, studies have shown that overexpression of GRAB sensors does not alter the cellular transcriptome in the mouse cortex, nor does it affect the expression level and localization of native GPCRs [61]. Additionally, no significant behavioral differences were observed in multiple behavioral tests between rodents expressing control fluorescent protein and those expressing GRAB sensors [49,50]. Together, these findings indicate that GRAB sensors have minimal impact on native neuromodulator signaling and enable reliable monitoring of neuromodulator dynamics without disrupting normal cellular physiology or animal behaviors.

In summary, PBP- and GPCR-based sensors offer complementary performance landscapes: PBP-based sensors provide robust responses *in vitro* and possess high-throughput optimization potential but may be limited by the availability of natural scaffolds and suboptimal membrane targeting capability in mammalian systems; GPCR-based sensors excel in physiological specificity and natural affinity for diverse neuromodulators, albeit with moderate kinetics; and chemigenetic sensors further push the boundaries of spectral diversity and dynamic range by leveraging superior synthetic fluorophores.

Recent progress of fluorescent neuromodulator sensors

Monoamine neuromodulators sensors

Monoamine neuromodulators, including dopamine (DA), norepinephrine/noradrenaline (NE/NA), 5-HT, and histamine (HA), constitute a critical class of signaling molecules in the nervous system. Despite their shared structural similarities, monoamine neuromodulators exhibit distinct receptor systems and functional specificities. DA is mainly associated with reward processing, motivation, and motor function, with its dysregulation linked to Parkinson's disease, addiction, and schizophrenia [74–77]. NE plays a key role in the regulation of stress responses, attention, and cardiovascular function [78,79]. 5-HT modulates mood, appetite, and sleep, and its dysfunction is associated with a range of psychiatric disorders, including depression and anxiety [80–82]. HA contributes to immune responses, sleep-wake cycles, and cognitive function [83–85]. To

better study their roles in both physiological and pathological processes, there is a need for tools that can sensitively and specifically monitor the activity of individual monoamines in real-time, particularly in living organisms engaged in complex behaviors.

Dopamine sensors. In 2018, Sun et al. [39] and Patriarchi et al. [40] independently developed the first-generation green fluorescent DA sensors, GRAB_{DA} and dLight, respectively, which were constructed by fusing circularly permuted enhanced green fluorescent protein (cpEGFP) to different DA receptor subtypes. These sensors enabled the first precise, specific, and real-time monitoring of endogenously released DA *in vivo* across species including fruit flies, zebrafish, and mice. In 2020, both teams [42,43] further expanded the spectral properties of DA sensors by using circularly permuted red fluorescent protein (cpmApple) to develop red fluorescent DA sensors. Sun et al. [42] developed rDA1m (medium DA affinity) and rDA1h (high DA affinity), which exhibit compatibility with green fluorescent calcium or neuromodulator sensors, enabling the simultaneous capture of dual neural signals in complex neural circuits. Furthermore, their red-shifted excitation wavelength confers superior *in vivo* optical performance, including enhanced tissue penetration depth, reduced background autofluorescence, and minimized phototoxicity, making these sensors ideal for multi-channel imaging studies. The same study also introduced the second-generation green fluorescent GRAB_{DA} sensors (DA2m and DA2h), which demonstrated a 2–3-fold maximum increase in fluorescence response amplitude compared to the first-generation sensors, substantially improving sensitivity [42].

In 2024, Zhuo et al. [49] further optimized the green and red GRAB_{DA} sensors through comprehensive scaffold screening of dopamine receptors from different species and rational site-directed mutagenesis combined with high-throughput cell-based screening, obtaining the third-generation green (DA3m and DA3h) and red fluorescent (rDA3m and rDA3h) sensors. Utilizing these ultra-sensitive GRAB_{DA} sensors, researchers were able to achieve spatially resolved detection of trace DA release in the cortex of mice engaged in various behavioral tasks. The development and *in vivo* application of this diverse family of DA sensors have significantly advanced the understanding of DA's role in reward processing, learning, and motor control [49].

In addition to the green and red channels, the availability of a third fluorescent imaging channel would enable the simultaneous observation of three distinct neural signals during behavior, providing a more comprehensive picture of neuromodulator interactions. To achieve this goal, Zheng et al. [52] developed the first far-red chemigenetic fluorescent GRAB_{DA} sensor HaloDA1.0, which incorporates cpHaloTag into the GRAB strat-

egy. Labeled with synthetic rhodamine dyes via the HaloTag ligand (HTL), HaloDA1.0 possesses far-red emission spectra. When used in conjunction with existing green and red sensors, it enables multicolor monitoring of dopamine (DA) alongside other neurochemicals and intracellular signaling *in vivo* (Figure 1D). This facilitates the study of crosstalk among multiple neuromodulators and complex neural circuits in living animals [52].

Norepinephrine/noradrenaline and octopamine sensors. In 2019, Feng et al. [41] developed the first-generation green fluorescent GRAB_{NE} sensors, enabling the real-time detection of endogenously released NE in both zebrafish and mice under optogenetic and behavioral stimulations. In 2023, Kagiampaki et al. [47] reported green and red norepinephrine sensors, nLightG and nLightR, with improved ligand selectivity derives from the sperm whale Alpha-1 adrenergic receptor scaffold. In 2024, Feng et al. [48] further optimized GRAB_{NE} sensors, producing the second-generation NE2m and NE2h, with differing affinities and improved brightness and sensitivity, demonstrated superior performance both *in vitro* and *in vivo*. Using NE2m and NE2h, researchers could precisely monitor NE dynamics in key brain regions such as the locus coeruleus (LC) and hypothalamus of freely moving mice. To enable more versatile use and further enhance multi-channel imaging capabilities, the team also developed Cre-dependent transgenic mice co-expressing green fluorescent NE2m and the red fluorescent calcium indicator jRGECO1a (Rosa26-CAG-LSL-jRGECO1a-iP2A-NE2m). Using these transgenic mice, they successfully recorded the dynamic changes of cortical NE release and calcium signaling simultaneously via mesoscopic imaging during sleep-wake cycles, sensory processing, and motor behaviors, advancing the understanding of NE's diverse roles in neural circuits [48].

Octopamine (OA), a structurally related monoamine neuromodulator predominantly found in invertebrates, is considered the functional analog of NE in vertebrates. It plays essential roles in regulating physiology and behavior, including olfactory associative learning. Lv et al. [51] reported a green fluorescent GRAB_{OA} sensor OA1.0, and successfully applied it to monitor *in vivo* OA release during an aversive learning paradigm in the mushroom body—an essential learning center in fruit flies—providing valuable perspectives on the cellular and circuit mechanisms underpinning OA signaling.

Serotonin sensors. In 2021, Wan et al. [44] developed the first-generation green fluorescent GRAB_{5-HT} sensor 5-HT1.0 based on the endogenous 5-HT receptor HTR2C following the GRAB sensor strategy. At around the same time, several other 5-HT sensors were also reported, including

iSeroSnFR [28], PsychLight [45], and sDarken [86]. However, these sensors exhibited certain limitations, such as small fluorescence response amplitudes, low sensitivity, or suboptimal molecular specificity, which constrained their effectiveness in complex *in vivo* applications. In 2024, Deng et al. [50] introduced the next generation of green fluorescent GRAB_{5-HT} sensor g5-HT3.0 through systematic protein engineering optimizations. Alongside this, they expanded the spectral palette by creating the red fluorescent r5-HT1.0 sensor. Through fiber photometry recording, these newly developed sensors with enhanced sensitivity enable the capture 5-HT release in distinct subcortical regions in freely moving mice. Moreover, mesoscopic imaging using these sensors uncovers the release patterns and dynamic changes of 5-HT in the mouse cortex with high spatiotemporal resolution under diverse physiological and pathological conditions, including seizure-induced neurochemical waves [50].

Histamine sensors. In 2023, Dong et al. [46] developed two green fluorescent GRAB_{HA} sensors, HA1m and HA1h, with different affinities. These sensors exhibit excellent photostability, nanomolar-level sensitivity, high specificity, and sub-second response kinetics, enabling real-time monitoring of histamine release. In acute mouse brain slices, these sensors successfully monitored histamine release induced by electrical stimulation. Furthermore, in freely moving mice, they revealed dynamic histamine release in the preoptic area of the hypothalamus (POA) and the medial prefrontal cortex (mPFC) during sleep-wake transitions, highlighting region-specific regulation of histamine signaling. These novel GRAB_{HA} sensors can help to further elucidate the role of histamine in health and disease, with broad application prospects [46].

Acetylcholine sensors

ACh is involved in regulating a wide range of physiological functions, including muscle contraction, cardiovascular function, synaptic plasticity, attention, and memory formation [87,88]. Jing et al. [37] first developed the green fluorescent sensor GACH2.0 (abbreviated as ACh2.0) by combining the human muscarinic ACh receptor M3R with cpEGFP. ACh2.0 can selectively respond to physiological concentrations of ACh, and has been successfully applied to detect the endogenous cholinergic transmission across various model organisms. In 2020, Borden et al. [26] reported a PBP-based ACh fluorescent sensor, iAChSnFR. However, its sensitivity and signal-to-noise ratio for detecting endogenous ACh release were relatively limited, which constrained its use *in vivo*. Subsequently, Jing et al. [38] further improved the GRAB_{ACh} sensor, leading to the optimized ACh3.0 version. ACh3.0 was used to reveal spatially distinct cholinergic signal patterns in the olfactory center of transgenic fruit flies, especially in response to exter-

nal stimuli such as odor and electric shocks. Furthermore, by employing techniques such as fiber photometry and two-photon imaging, the authors successfully monitored dynamic changes of ACh release in multiple brain regions of freely behaving mice under different behavioral conditions [38]. These novel GRAB_{ACh} sensors open new avenues for dissecting the spatiotemporal dynamics and regulatory mechanisms of cholinergic signaling in complex neural circuits.

Purines sensors

Purine neuromodulators, mainly adenosine 5'-triphosphate (ATP) and adenosine (Ado), play critical roles in the nervous system. Beyond its canonical role as a cellular energy carrier, ATP also serves as an extracellular signaling molecule that participates in processes like pain perception and mechanosensory transmission [89–91]. Abnormal signaling of ATP is implicated in a variety of pathological processes [92,93]. Ado, on the other hand, is important for modulating physiological functions such as sleep-wake cycles, learning and memory, cardiovascular function, and immune responses [94–96]. Dysregulation of Ado signaling is closely associated with disorders including epilepsy, stroke, and neurodegenerative diseases. The PBP-based iATPSnFR [27] were effective for detecting intracellular ATP changes with high spatiotemporal resolution, but its relatively limited sensitivity and signal-to-noise ratio restricted their utility for monitoring extracellular ATP *in vivo*. To overcome this, Wu et al. developed green fluorescent GRAB sensors ATP1.0 [54] and Ado1.0 [53], enabling real-time monitoring of extracellular ATP and Ado dynamics with high specificity. ATP1.0 successfully captured spontaneous and stimulus-evoked ATP release in hippocampal primary neuronal cultures, injury-induced ATP release in zebrafish models, and ATP secretion from astrocytes in the cortex of lipopolysaccharide (LPS)-treated mice [54]. Studies using Ado1.0 revealed rapid, neuronal activity-dependent increases in extracellular Ado concentration in the basal forebrain (BF), a brain region critical for regulating arousal and sleep-wake transitions [53].

Additionally, Umpierre et al. [56] applied the green fluorescent GRAB sensor UDP1.0 to discover that uridine diphosphate (UDP) release may represent a conserved response of different brain regions to epilepsy and excitotoxic conditions. This finding provides new insights into the role of UDP in pathological processes within the nervous system and opens avenues for further research into its functional significance.

Lipid neuromodulator sensors

Endocannabinoids sensors. Endocannabinoids (eCBs) are crucial retrograde neuromodulators that

influence synaptic plasticity, emotion, pain perception, and sleep-wake cycles [97–99]. Dong et al. [57] developed the GRAB_{eCB} sensor eCB2.0 by inserting cpEGFP into the human cannabinoid receptor CB1R. This sensor enables real-time monitoring of dynamic eCB changes *in vivo* with high spatiotemporal resolution. In epilepsy models, eCB2.0 captured the propagation of eCB waves in the hippocampus alongside calcium waves, providing insights into the role of eCBs during pathological activity and revealing novel dynamic features of eCB signaling [57].

Prostaglandins sensors. Prostaglandins (PGs) are a diverse group of lipid signaling molecules involved in inflammation, sleep regulation, and other physiological processes [100–102]. Among them, prostaglandin D2 (PGD2) is notable for its roles in sleep regulation and immune responses. Sang et al. [58] reported the green fluorescent GRAB_{PGD2} sensor PGD2-1.0, based on the PGD2 receptor type 1. This sensor successfully detected the significant increase of PGD2 in the brain during sleep deprivation, revealing connections between inflammation and sleep. The development of sensors for specific lipid molecules such as PGD2 illustrates the importance and the corresponding challenges of achieving high molecular specificity and selectivity for studying lipid neuromodulator signaling *in vivo* [58].

Neuropeptide sensors

Neuropeptides, initially discovered as endocrine signaling molecules nearly 70 years ago, are now recognized as critical neuromodulators in the central and peripheral nervous systems [4]. They influence digestion, metabolism, reproduction, circadian rhythms, sleep, and higher cognitive functions [103–108]. Since neuropeptide signaling primarily relies on GPCRs, the GRAB strategy offers clear advantages for sensor design.

In 2023, Qian et al. [59] developed a GRAB sensor for oxytocin (OT), which not only enabled the visualization of the compartmental release of OT and elucidated the underlying molecular mechanism, but also facilitates real-time *in vivo* monitoring of OT dynamics during innate behaviors. Wang et al. [61] used the GRAB strategy combined with a grafting approach to efficiently develop a tool kit of green fluorescent neuropeptide sensors. These sensors can detect nanomolar levels of various neuropeptides, including somatostatin (SST), corticotropin-releasing factor (CRF), cholecystokinin (CCK), neuropeptide Y (NPY), neurotensin (NTS), and vasoactive intestinal peptide (VIP). *In vivo* applications demonstrated real-time monitoring of SST and CRF dynamics in behaving animals, helping reveal their functional roles in neural circuits [61]. For hypocretin/orexin (Hcrt/OX), a GRAB_{Hcrt/OX} sensor was employed to detect elevated levels in mice during novel object-place exploration, aim-

ing to elucidate the role of Hcrt/OX in spatial memory [64]. These fluorescent sensors provide powerful tools to explore how neuropeptide signaling regulates physiology and behavior under normal and pathological conditions.

Parallel efforts have also advanced the development of neuropeptide sensors. Duffet et al. [66] developed OxLight1, another fluorescent sensor based on the human OX2R receptor, enabling detection of Hcrt/OX release linked to spontaneous locomotion, acute stress, and sleep-wake transitions in mice. Ino et al. [60] developed MTRIA_{OT}, a sensor built from the medaka fish OT receptor, which successfully reported social interaction-induced OT signals during *in vivo* recording. In 2023, Duffet et al. [67] introduced GLPLight1, based on the human glucagon-like peptide-1 (GLP-1) receptor GLP1R, aiming for detecting GLP-1 and its derivatives, although its capacity to monitor endogenous GLP-1 release *in vivo* remains to be fully validated.

Opioid neuropeptides regulate key processes such as pain perception, reward, and aversion by activating κ , δ , and μ opioid receptors (κ OR, δ OR, and μ OR), which have significant clinical implications [109–111]. Dong et al. [69] developed a family of genetically encoded fluorescent sensors based on different opioid receptors, namely κ Light, δ Light, and μ Light. In mouse experiments, these sensors detected rapid, subregion-specific opioid peptide release in the nucleus accumbens (NAc) during fear- and reward-related behaviors, uncovering distinct release patterns linked to behavioral states. Nociceptin/orphanin FQ (N/OFFQ) is another opioid neuropeptide with important roles in regulating stress, feeding, sleep, and motivation [112,113]. Zhou et al. [68] developed the fluorescent sensor NOPLight, which captured the N/OFFQ release dynamics in tissues and freely behaving animals. These tools pave the way for new studies into the roles of opioid neuropeptides in behavior and disease.

Extending these advances beyond mammals, Xia and Li [65] developed the green fluorescent GRAB sensor sNPF1.0 for detecting short neuropeptide F (sNPF) in fruit flies. By using sNPF1.0 and ACh3.0 sensors, they uncovered differences in spatiotemporal release dynamics and molecular regulation of sNPF and ACh release. These findings highlight the versatility of GRAB sensors for studying diverse neuromodulators, from classical neurotransmitters to neuropeptides, across multiple species [65].

Future directions

Genetically encoded fluorescent sensors for neuromodulators have revolutionized neuroscience research by enabling real-time, dynamic monitoring of the release and fluctuations of diverse neuromodulators *in vivo*. When

selecting specific fluorescent sensors for neuromodulators, it is also necessary to consider the characteristics of different versions, such as fluorescence response amplitude, affinity, and the pharmacological properties of the scaffold proteins. With the continuous improvement of the signal-to-noise ratio and the expansion of the range of detectable molecules, we will be able to achieve more comprehensive analysis of a wider range of neuromodulators within complex biological contexts. This will provide strong support for basic neuroscience research, exploration of disease mechanisms, and the development of neuropharmacological agents.

The interplay between neurotransmitter and neuromodulator systems is highly prevalent and physiologically relevant in the nervous system [114], highlighting the need for simultaneous monitoring of multiple neuromodulators in intact neural circuits. The development of chemigenetic sensors with far-red or near-infrared emission will enhance multiplexing capabilities, thereby enabling real-time visualization of neuromodulatory interactions and crosstalk within the same experimental preparation. Deploying sensors with distinct emission spectra enables concurrent detection of several neuromodulators, e.g., DA, ACh, 5-HT, and eCBs—alongside downstream signaling readouts such as intracellular calcium ($[Ca^{2+}]_i$) and cyclic adenosine 5'-monophosphate (cAMP)—revealing intricate neurochemical network crosstalk during spontaneous, internally generated behaviors unconstrained by external cues or fixed timing in the same mouse. By incorporating additional protein tags and bioavailable chemical dyes with distinct spectra, simultaneous four-color (or even more colors) recording *in vivo* will be achievable in the future.

Another emerging need in neuromodulator research is qualitative or semi-quantitative measurement. The physiological concentration of neuromodulators across different brain regions and states are tightly regulated and related to normal function. Critically, determining their levels is essential for studying the pathology and treatment of neurological disorders—such as DA in Parkinson's disease (PD) and 5-HT in major depressive disorder (MDD). To address this, the development of fluorescent lifetime-based sensors holds great promise for more quantitative measurements of neuromodulator dynamics in animal models. Unlike intensimetric sensors, which can be influenced by expression levels, light scattering and absorption, as well as the imaging parameters, the lifetime-based sensors offer more robust and accurate readouts, which make them ideal for longitudinal and comparative studies. With appropriate instrumentation and analytical methods, fluorescent lifetime-based sensors

could, for instance, be used to quantitatively track DA depletion process in the substantia nigra in PD models, enabling precise assessments of disease progression and valuable insights for understanding pathophysiology and guiding the development of more effective therapeutics. For practical implementation, developing high-throughput screening methods to facilitate the ongoing optimization of next-generation neuromodulator sensors is also necessary. A well-designed rational screening strategy will further expand the sensor toolkit to include chemigenetic sensors and fluorescent lifetime-based sensors.

CRediT authorship contribution statement

Shengwei Fu: Writing – review & editing, Writing – original draft. **Yulong Li:** Writing – review & editing, Writing – original draft.

DATA AVAILABILITY

No data was used for the research described in the article.

DECLARATION OF COMPETING INTEREST

The authors declare that they have no known competing financial interests or personal relationships that could have appeared to influence the work reported in this paper.

Acknowledgments

This work was supported by the National Major Project of China Science and Technology Innovation 2030 for Brain Science and Brain-Inspired Technology (2022ZD0205600), the National Key Research and Development Program of China (2022YFE0108700, 2023YFE0207100), the National Natural Science Foundation of China (32525003), and the Beijing Municipal Science & Technology Commission (Z220009). Support was also provided by the Peking-Tsinghua Center for Life Sciences, the State Key Laboratory of Membrane Biology at Peking University School of Life Sciences, the Feng Foundation of Biomedical Research, the Clement and Xinxin Foundation, and the New Cornerstone Science Foundation through the New Cornerstone Investigator Program (to Y.L.).

Received 30 November 2025;

Accepted 26 January 2026;

Available online 30 January 2026

Keywords:
 neuromodulation;
 genetically encoded fluorescent sensors;
 neuromodulator sensors;
 fluorescence imaging

References

- [1]. Luo, L., (2021). Architectures of neuronal circuits. *Science* **373**, eabg7285. <https://doi.org/10.1126/science.abg7285>.
- [2]. Südhof, T.C., Release, N., (2008). In: *Pharmacology of Neurotransmitter Release*. Springer, Berlin, Heidelberg, pp. 1–21. https://doi.org/10.1007/978-3-540-74805-2_1.
- [3]. Marder, E., (2012). Neuromodulation of neuronal circuits: back to the future. *Neuron* **76**, 1–11. <https://doi.org/10.1016/j.neuron.2012.09.010>.
- [4]. van den Pol, A.N., (2012). Neuropeptide transmission in brain circuits. *Neuron* **76**, 98–115. <https://doi.org/10.1016/j.neuron.2012.09.014>.
- [5]. Krishnan, V., Nestler, E.J., (2008). The molecular neurobiology of depression. *Nature* **455**, 894–902. <https://doi.org/10.1038/nature07455>.
- [6]. Malhi, G.S., Mann, J.J., (2018). Depression. *Lancet* **392**, 2299–2312. [https://doi.org/10.1016/S0140-6736\(18\)31948-2](https://doi.org/10.1016/S0140-6736(18)31948-2).
- [7]. Grace, A.A., (2016). Dysregulation of the dopamine system in the pathophysiology of schizophrenia and depression. *Nature Rev. Neurosci.* **17**, 524–532. <https://doi.org/10.1038/nrn.2016.57>.
- [8]. McCutcheon, R.A., Reis Marques, T., Howes, O.D., (2020). Schizophrenia—an overview. *JAMA Psychiat.* **77**, 201–210. <https://doi.org/10.1001/jamapsychiatry.2019.3360>.
- [9]. Barone, P., (2010). Neurotransmission in Parkinson's disease: beyond dopamine. *Eur. J. Neurol.* **17**, 364–376. <https://doi.org/10.1111/j.1468-1331.2009.02900.x>.
- [10]. Zucca, F.A., Segura-Aguilar, J., Ferrari, E., Muñoz, P., Paris, I., Sulzer, D., et al., (2017). Interactions of iron, dopamine and neuromelanin pathways in brain aging and Parkinson's disease. *Prog. Neurobiol.* **155**, 96–119. <https://doi.org/10.1016/j.pneurobio.2015.09.012>.
- [11]. Hampel, H., Mesulam, M.-M., Cuello, A.C., Farlow, M.R., Giacobini, E., Grossberg, G.T., et al., (2018). The cholinergic system in the pathophysiology and treatment of Alzheimer's disease. *Brain* **141**, 1917–1933. <https://doi.org/10.1093/brain/awy132>.
- [12]. Long, J.M., Holtzman, D.M., (2019). Alzheimer disease: an update on pathobiology and treatment strategies. *Cell* **179**, 312–339. <https://doi.org/10.1016/j.cell.2019.09.001>.
- [13]. Bito, L., Davson, H., Levin, E., Murray, M., Snider, N., (1966). The concentrations of free amino acids and other electrolytes in cerebrospinal fluid, vivo dialysate of brain, and blood plasma of the dog. *J. Neurochem.* **13**, 1057–1067. <https://doi.org/10.1111/j.1471-4159.1966.tb04265.x>.
- [14]. Hogan, B.L., Lunte, S.M., Stobaugh, J.F., Lunte, C.E., (1994). Online coupling of *in vivo* microdialysis sampling with capillary electrophoresis. *Anal. Chem.* **66**, 596–602. <https://doi.org/10.1021/ac00077a004>.
- [15]. Li, H., Li, C., Yan, Z., Yang, J., Chen, H., (2010). Simultaneous monitoring multiple neurotransmitters and neuromodulators during cerebral ischemia/reperfusion in rats by microdialysis and capillary electrophoresis. *J. Neurosci. Methods* **189**, 162–168. <https://doi.org/10.1016/j.jneumeth.2010.03.022>.
- [16]. Adams, R.N., (1976). Probing brain chemistry with electroanalytical. *Anal. Chem.* **48**, 1128A–1138A. <https://doi.org/10.1021/ac50008a713>.
- [17]. Stamford, J.A., Kruk, Z.L., Millar, J., Wightman, R.M., (1984). Striatal dopamine uptake in the rat: *in vivo* analysis by fast cyclic voltammetry. *Neurosci. Letters* **51**, 133–138. [https://doi.org/10.1016/0304-3940\(84\)90274-X](https://doi.org/10.1016/0304-3940(84)90274-X).
- [18]. Bucher, E.S., Wightman, R.M., (2015). Electrochemical analysis of neurotransmitters. *Annu. Rev. Anal. Chem.* **8**, 239–261. <https://doi.org/10.1146/annurev-anchem-071114-040426>.
- [19]. Kissinger, P.T., Hart, J.B., Adams, R.N., (1973). Voltammetry in brain tissue – a new neurophysiological measurement. *Brain Res.* **55**, 209–213. [https://doi.org/10.1016/0006-8993\(73\)90503-9](https://doi.org/10.1016/0006-8993(73)90503-9).
- [20]. Lin, M.Z., Schnitzer, M.J., (2016). Genetically encoded indicators of neuronal activity. *Nature Neurosci.* **19**, 1142–1153. <https://doi.org/10.1038/nn.4359>.
- [21]. Wu, Z., Lin, D., Li, Y., (2022). Pushing the frontiers: tools for monitoring neurotransmitters and neuromodulators. *Nature Rev. Neurosci.* **23**, 257–274. <https://doi.org/10.1038/s41583-022-00577-6>.
- [22]. Okumoto, S., Looger, L.L., Micheva, K.D., Reimer, R.J., Smith, S.J., Frommer, W.B., (2005). Detection of glutamate release from neurons by genetically encoded surface-displayed FRET nanosensors. *PNAS* **102**, 8740–8745. <https://doi.org/10.1073/pnas.0503274102>.
- [23]. Marvin, J.S., Borghuis, B.G., Tian, L., Cichon, J., Harnett, M.T., Akerboom, J., et al., (2013). An optimized fluorescent probe for visualizing glutamate neurotransmission. *Nature Methods* **10**, 162–170. <https://doi.org/10.1038/nmeth.2333>.
- [24]. Marvin, J.S., Scholl, B., Wilson, D.E., Podgorski, K., Kazemipour, A., Müller, J.A., et al., (2018). Stability, affinity, and chromatic variants of the glutamate sensor iGluSnFR. *Nature Methods* **15**, 936–939. <https://doi.org/10.1038/s41592-018-0171-3>.
- [25]. Aggarwal, A., Liu, R., Chen, Y., Ralowicz, A.J., Bergerson, S.J., Tomaska, F., et al., (2023). Glutamate indicators with improved activation kinetics and localization for imaging synaptic transmission. *Nature Methods* **20**, 925–934. <https://doi.org/10.1038/s41592-023-01863-6>.
- [26]. Borden, P.M., Zhang, P., Shivange, A.V., Marvin, J.S., Cichon, J., Dan, C., et al., (2020). A fast genetically encoded fluorescent sensor for faithful *in vivo* acetylcholine detection in mice, fish, worms and flies. *bioRxiv* 2020.02.07.939504. <https://doi.org/10.1101/2020.02.07.939504>.
- [27]. Lobas, M.A., Tao, R., Nagai, J., Kronschräger, M.T., Borden, P.M., Marvin, J.S., et al., (2019). A genetically encoded single-wavelength sensor for imaging cytosolic and cell surface ATP. *Nature Commun.* **10**, 711. <https://doi.org/10.1038/s41467-019-08441-5>.
- [28]. Unger, E.K., Keller, J.P., Altermatt, M., Liang, R., Matsui, A., Dong, C., et al., (2020). Directed evolution of a selective and sensitive serotonin sensor via machine learning. *Cell* **183**, 1986–2002.e26. <https://doi.org/10.1016/j.cell.2020.11.040>.

- [29]. McCorvy, J.D., Roth, B.L., (2015). Structure and function of serotonin G protein-coupled receptors. *Pharmacol. Ther.* **150**, 129–142. <https://doi.org/10.1016/j.pharmthera.2015.01.009>.
- [30]. Sharp, T., Barnes, N.M., (2020). Central 5-HT receptors and their function; present and future. *Neuropharmacology* **177**, 108155. <https://doi.org/10.1016/j.neuropharm.2020.108155>.
- [31]. Gether, U., Lin, S., Kobilka, B.K., (1995). Fluorescent labeling of purified β_2 adrenergic receptor. *J. Biol. Chem.* **270**, 28268–28275. <https://doi.org/10.1074/jbc.270.47.28268>.
- [32]. Rasmussen, S.G.F., Choi, H.-J., Rosenbaum, D.M., Kobilka, T.S., Thian, F.S., Edwards, P.C., et al., (2007). Crystal structure of the human β_2 adrenergic G-protein-coupled receptor. *Nature* **450**, 383–387. <https://doi.org/10.1038/nature06325>.
- [33]. Cherezov, V., Rosenbaum, D.M., Hanson, M.A., Rasmussen, S.G.F., Thian, F.S., Kobilka, T.S., et al., (2007). High-resolution crystal structure of an engineered human β_2 -adrenergic G protein-coupled receptor. *Science* **318**, 1258–1265. <https://doi.org/10.1126/science.1150577>.
- [34]. Jaakola, V.-P., Griffith, M.T., Hanson, M.A., Cherezov, V., Chien, E.Y.T., Lane, J.R., et al., (2008). The 2.6 Angstrom crystal structure of a human A2A adenosine receptor bound to an antagonist. *Science* **322**, 1211–1217. <https://doi.org/10.1126/science.1164772>.
- [35]. Haga, K., Kruse, A.C., Asada, H., Yurugi-Kobayashi, T., Shiroishi, M., Zhang, C., et al., (2012). Structure of the human M2 muscarinic acetylcholine receptor bound to an antagonist. *Nature* **482**, 547–551. <https://doi.org/10.1038/nature10753>.
- [36]. Huang, W., Manglik, A., Venkatakrisnan, A.J., Laeremans, T., Feinberg, E.N., Sanborn, A.L., et al., (2015). Structural insights into μ -opioid receptor activation. *Nature* **524**, 315–321. <https://doi.org/10.1038/nature14886>.
- [37]. Jing, M., Zhang, P., Wang, G., Feng, J., Mesik, L., Zeng, J., et al., (2018). A genetically encoded fluorescent acetylcholine indicator for *in vitro* and *in vivo* studies. *Nature Biotechnol.* **36**, 726–737. <https://doi.org/10.1038/nbt.4184>.
- [38]. Jing, M., Li, Y., Zeng, J., Huang, P., Skirzewski, M., Kljakic, O., et al., (2020). An optimized acetylcholine sensor for monitoring *in vivo* cholinergic activity. *Nature Methods* **17**, 1139–1146. <https://doi.org/10.1038/s41592-020-0953-2>.
- [39]. Sun, F., Zeng, J., Jing, M., Zhou, J., Feng, J., Owen, S. F., et al., (2018). A genetically encoded fluorescent sensor enables rapid and specific detection of dopamine in flies, fish, and mice. *Cell* **174**, 481–496.e19. <https://doi.org/10.1016/j.cell.2018.06.042>.
- [40]. Patriarchi, T., Cho, J.R., Merten, K., Howe, M.W., Marley, A., Xiong, W.-H., et al., (2018). Ultrafast neuronal imaging of dopamine dynamics with designed genetically encoded sensors. *Science* **360**, eaat4422. <https://doi.org/10.1126/science.aat4422>.
- [41]. Feng, J., Zhang, C., Lischinsky, J.E., Jing, M., Zhou, J., Wang, H., et al., (2019). A genetically encoded fluorescent sensor for rapid and specific *in vivo* detection of norepinephrine. *Neuron* **102**, 745–761.e8. <https://doi.org/10.1016/j.neuron.2019.02.037>.
- [42]. Sun, F., Zhou, J., Dai, B., Qian, T., Zeng, J., Li, X., et al., (2020). Next-generation GRAB sensors for monitoring dopaminergic activity *in vivo*. *Nature Methods* **17**, 1156–1166. <https://doi.org/10.1038/s41592-020-00981-9>.
- [43]. Patriarchi, T., Mohebi, A., Sun, J., Marley, A., Liang, R., Dong, C., et al., (2020). An expanded palette of dopamine sensors for multiplex imaging *in vivo*. *Nature Methods* **17**, 1147–1155. <https://doi.org/10.1038/s41592-020-0936-3>.
- [44]. Wan, J., Peng, W., Li, X., Qian, T., Song, K., Zeng, J., et al., (2021). A genetically encoded sensor for measuring serotonin dynamics. *Nature Neurosci.* **24**, 746–752. <https://doi.org/10.1038/s41593-021-00823-7>.
- [45]. Dong, C., Ly, C., Dunlap, L.E., Vargas, M.V., Sun, J., Hwang, I.-W., et al., (2021). Psychedelic-inspired drug discovery using an engineered biosensor. *Cell* **184**, 2779–2792.e18. <https://doi.org/10.1016/j.cell.2021.03.043>.
- [46]. Dong, H., Li, M., Yan, Y., Qian, T., Lin, Y., Ma, X., et al., (2023). Genetically encoded sensors for measuring histamine release both *in vitro* and *in vivo*. *Neuron* **111**, 1564–1576.e6. <https://doi.org/10.1016/j.neuron.2023.02.024>.
- [47]. Kagiampaki, Z., Rohner, V., Kiss, C., Curreli, S., Dieter, A., Wilhelm, M., et al., (2023). Sensitive multicolor indicators for monitoring norepinephrine *in vivo*. *Nature Methods* **20**, 1426–1436. <https://doi.org/10.1038/s41592-023-01959-z>.
- [48]. Feng, J., Dong, H., Lischinsky, J.E., Zhou, J., Deng, F., Zhuang, C., et al., (2024). Monitoring norepinephrine release *in vivo* using next-generation GRABNE sensors. *Neuron* **112**, 1930–1942.e6. <https://doi.org/10.1016/j.neuron.2024.03.001>.
- [49]. Zhuo, Y., Luo, B., Yi, X., Dong, H., Miao, X., Wan, J., et al., (2024). Improved green and red GRAB sensors for monitoring dopaminergic activity *in vivo*. *Nature Methods* **21**, 680–691. <https://doi.org/10.1038/s41592-023-02100-w>.
- [50]. Deng, F., Wan, J., Li, G., Dong, H., Xia, X., Wang, Y., et al., (2024). Improved green and red GRAB sensors for monitoring spatiotemporal serotonin release *in vivo*. *Nature Methods* **21**, 692–702. <https://doi.org/10.1038/s41592-024-02188-8>.
- [51]. Lv, M., Cai, R., Zhang, R., Xia, X., Li, X., Wang, Y., et al., (2024). An octopamine-specific GRAB sensor reveals a monoamine relay circuitry that boosts aversive learning. *Natl. Sci. Rev.* **11**, nwae112. <https://doi.org/10.1093/nsr/nwae112>.
- [52]. Zheng, Y., Cai, R., Wang, K., Zhang, J., Zhuo, Y., Dong, H., et al., (2025). *In vivo* multiplex imaging of dynamic neurochemical networks with designed far-red dopamine sensors. *Science*. <https://doi.org/10.1126/science.adt7705>.
- [53]. Peng, W., Wu, Z., Song, K., Zhang, S., Li, Y., Xu, M., (2020). Regulation of sleep homeostasis mediator adenosine by basal forebrain glutamatergic neurons. *Science* **369**, eabb0556. <https://doi.org/10.1126/science.abb0556>.
- [54]. Wu, Z., He, K., Chen, Y., Li, H., Pan, S., Li, B., et al., (2022). A sensitive GRAB sensor for detecting

- extracellular ATP *in vitro* and *in vivo*. *Neuron* **110**, 770–782.e5. <https://doi.org/10.1016/j.neuron.2021.11.027>.
- [55]. Wu, Z., Cui, Y., Wang, H., Wu, H., Wan, Y., Li, B., et al., (2023). Neuronal activity-induced, equilibrative nucleoside transporter-dependent, somatodendritic adenosine release revealed by a GRAB sensor. *PNAS* **120**, e2212387120. <https://doi.org/10.1073/pnas.2212387120>.
- [56]. Umpierre, A.D., Li, B., Ayasoufi, K., Simon, W.L., Zhao, S., Xie, M., et al., (2024). Microglial P2Y6 calcium signaling promotes phagocytosis and shapes neuroimmune responses in epileptogenesis. *Neuron* **112**, 1959–1977.e10. <https://doi.org/10.1016/j.neuron.2024.03.017>.
- [57]. Dong, A., He, K., Dudok, B., Farrell, J.S., Guan, W., Liput, D.J., et al., (2022). A fluorescent sensor for spatiotemporally resolved imaging of endocannabinoid dynamics *in vivo*. *Nature Biotechnol.* **40**, 787–798. <https://doi.org/10.1038/s41587-021-01074-4>.
- [58]. Sang, D., Lin, K., Yang, Y., Ran, G., Li, B., Chen, C., et al., (2023). Prolonged sleep deprivation induces a cytokine-storm-like syndrome in mammals. *Cell* **186**, 5500–5516.e21. <https://doi.org/10.1016/j.cell.2023.10.025>.
- [59]. Qian, T., Wang, H., Wang, P., Geng, L., Mei, L., Osakada, T., et al., (2023). A genetically encoded sensor measures temporal oxytocin release from different neuronal compartments. *Nature Biotechnol.* **41**, 944–957. <https://doi.org/10.1038/s41587-022-01561-2>.
- [60]. Ino, D., Tanaka, Y., Hibino, H., Nishiyama, M., (2022). A fluorescent sensor for real-time measurement of extracellular oxytocin dynamics in the brain. *Nature Methods* **19**, 1286–1294. <https://doi.org/10.1038/s41592-022-01597-x>.
- [61]. Wang, H., Qian, T., Zhao, Y., Zhuo, Y., Wu, C., Osakada, T., et al., (2023). A tool kit of highly selective and sensitive genetically encoded neuropeptide sensors. *Science* **382**, eabq8173. <https://doi.org/10.1126/science.abq8173>.
- [62]. Li, H., Namburi, P., Olson, J.M., Borio, M., Lemieux, M. E., Beyeler, A., et al., (2022). Neurotensin orchestrates valence assignment in the amygdala. *Nature* **608**, 586–592. <https://doi.org/10.1038/s41586-022-04964-y>.
- [63]. Ono, D., Wang, H., Hung, C.J., Wang, H., Kon, N., Yamanaka, A., et al., (2023). Network-driven intracellular cAMP coordinates circadian rhythm in the suprachiasmatic nucleus. *Sci. Adv.* **9**, eabq7032. <https://doi.org/10.1126/sciadv.abq7032>.
- [64]. Liao, Y., Wen, R., Fu, S., Cheng, X., Ren, S., Lu, M., et al., (2024). Spatial memory requires hypocretins to elevate medial entorhinal gamma oscillations. *Neuron* **112**, 155–173.e8. <https://doi.org/10.1016/j.neuron.2023.10.012>.
- [65]. Xia, X., Li, Y., (2025). A high-performance GRAB sensor reveals differences in the dynamics and molecular regulation between neuropeptide and neurotransmitter release. *Nature Commun.* **16**, 819. <https://doi.org/10.1038/s41467-025-56129-w>.
- [66]. Duffet, L., Kosar, S., Panniello, M., Viberti, B., Bracey, E., Zych, A.D., et al., (2022). A genetically encoded sensor for *in vivo* imaging of orexin neuropeptides. *Nature Methods* **19**, 231–241. <https://doi.org/10.1038/s41592-021-01390-2>.
- [67]. Duffet, L., Williams, E.T., Gresch, A., Chen, S., Bhat, M. A., Benke, D., et al., (2023). Optical tools for visualizing and controlling human GLP-1 receptor activation with high spatiotemporal resolution. *eLife* **12**, RP86628. <https://doi.org/10.7554/eLife.86628>.
- [68]. Zhou, X., Stine, C., Prada, P.O., Fusca, D., Assoumou, K., Deric, J., et al., (2024). Development of a genetically encoded sensor for probing endogenous nociceptin opioid peptide release. *Nature Commun.* **15**, 5353. <https://doi.org/10.1038/s41467-024-49712-0>.
- [69]. Dong, C., Gowrishankar, R., Jin, Y., He, X.J., Gupta, A., Wang, H., et al., (2024). Unlocking opioid neuropeptide dynamics with genetically encoded biosensors. *Nature Neurosci.* **27**, 1844–1857. <https://doi.org/10.1038/s41593-024-01697-1>.
- [70]. Deo, C., Abdelfattah, A.S., Bhargava, H.K., Berro, A.J., Falco, N., Farrants, H., et al., (2021). The HaloTag as a general scaffold for far-red tunable chemigenetic indicators. *Nature Chem. Biol.* **17**, 718–723. <https://doi.org/10.1038/s41589-021-00775-w>.
- [71]. Farrants, H., Shuai, Y., Lemon, W.C., Monroy Hernandez, C., Zhang, D., Yang, S., et al., (2024). A modular chemigenetic calcium indicator for multiplexed *in vivo* functional imaging. *Nature Methods* **21**, 1916–1925. <https://doi.org/10.1038/s41592-024-02411-6>.
- [72]. Frei, M.S., Sanchez, S.A., He, X., Liu, L., Schneider, F., Wang, Z., et al., (2025). Far-red chemigenetic kinase biosensors enable multiplexed and super-resolved imaging of signaling networks. *Nature Biotechnol.*, 1–10. <https://doi.org/10.1038/s41587-025-02642-8>.
- [73]. Lavis, L.D., (2017). Teaching old dyes new tricks: biological probes built from fluoresceins and rhodamines. *Annu. Rev. Biochem.* **86**, 825–843. <https://doi.org/10.1146/annurev-biochem-061516-044839>.
- [74]. Kalivas, P.W., Stewart, J., (1991). Dopamine transmission in the initiation and expression of drug- and stress-induced sensitization of motor activity. *Brain Res. Rev.* **16**, 223–244. [https://doi.org/10.1016/0165-0173\(91\)90007-U](https://doi.org/10.1016/0165-0173(91)90007-U).
- [75]. Wise, R.A., (2004). Dopamine, learning and motivation. *Nature Rev. Neurosci.* **5**, 483–494. <https://doi.org/10.1038/nrn1406>.
- [76]. Volkow, N.D., Wise, R.A., Baler, R., (2017). The dopamine motive system: implications for drug and food addiction. *Nature Rev. Neurosci.* **18**, 741–752. <https://doi.org/10.1038/nrn.2017.130>.
- [77]. Klein, M.O., Battagello, D.S., Cardoso, A.R., Hauser, D. N., Bittencourt, J.C., Correa, R.G., (2019). Dopamine: functions, signaling, and association with neurological diseases. *Cell. Mol. Neurobiol.* **39**, 31–59. <https://doi.org/10.1007/s10571-018-0632-3>.
- [78]. Moore, R.Y., Bloom, F.E., (1979). Central catecholamine neuron systems: anatomy and physiology of the norepinephrine and epinephrine systems. *Annu. Rev. Neurosci.* **2**, 113–168. <https://doi.org/10.1146/annurev.ne.02.030179.000553>.
- [79]. Schwarz, L.A., Luo, L., (2015). Organization of the locus coeruleus-norepinephrine system. *Curr. Biol.* **25**, R1051–R1056. <https://doi.org/10.1016/j.cub.2015.09.039>.
- [80]. Berger, M., Gray, J.A., Roth, B.L., (2009). The expanded biology of serotonin. *Annu. Rev. Med.* **60**, 355–366. <https://doi.org/10.1146/annurev.med.60.042307.110802>.
- [81]. Lesch, K.-P., Waider, J., (2012). Serotonin in the modulation of neural plasticity and networks: implications

- for neurodevelopmental disorders. *Neuron* **76**, 175–191. <https://doi.org/10.1016/j.neuron.2012.09.013>.
- [82]. Moncrieff, J., Cooper, R.E., Stockmann, T., Amendola, S., Hengartner, M.P., Horowitz, M.A., (2023). The serotonin theory of depression: a systematic umbrella review of the evidence. *Mol. Psychiatry* **28**, 3243–3256. <https://doi.org/10.1038/s41380-022-01661-0>.
- [83]. Brown, R.E., Stevens, D.R., Haas, H.L., (2001). The physiology of brain histamine. *Prog. Neurobiol.* **63**, 637–672. [https://doi.org/10.1016/S0301-0082\(00\)00039-3](https://doi.org/10.1016/S0301-0082(00)00039-3).
- [84]. Haas, H.L., Sergeeva, O.A., Selbach, O., (2008). Histamine in the nervous system. *Physiol. Rev.* **88**, 1183–1241. <https://doi.org/10.1152/physrev.00043.2007>.
- [85]. Jutel, M., Akdis, M., Akdis, C.A., (2009). Histamine, histamine receptors and their role in immune pathology. *Clin. Exp. Allergy* **39**, 1786–1800. <https://doi.org/10.1111/j.1365-2222.2009.03374.x>.
- [86]. Kubitschke, M., Müller, M., Wallhorn, L., Pulin, M., Mittag, M., Pollok, S., et al., (2022). Next generation genetically encoded fluorescent sensors for serotonin. *Nature Commun.* **13**, 7525. <https://doi.org/10.1038/s41467-022-35200-w>.
- [87]. Hasselmo, M.E., (2006). The role of acetylcholine in learning and memory. *Curr. Opin. Neurobiol.* **16**, 710–715. <https://doi.org/10.1016/j.conb.2006.09.002>.
- [88]. Picciotto, M.R., Higley, M.J., Mineur, Y.S., (2012). Acetylcholine as a neuromodulator: cholinergic signaling shapes nervous system function and behavior. *Neuron* **76**, 116–129. <https://doi.org/10.1016/j.neuron.2012.08.036>.
- [89]. Fields, R.D., Stevens, B., (2000). ATP: an extracellular signaling molecule between neurons and glia. *Trends Neurosci.* **23**, 625–633. [https://doi.org/10.1016/S0166-2236\(00\)01674-X](https://doi.org/10.1016/S0166-2236(00)01674-X).
- [90]. Burnstock, G., (2001). Purine-mediated signalling in pain and visceral perception. *Trends Pharmacol. Sci.* **22**, 182–188. [https://doi.org/10.1016/S0165-6147\(00\)01643-6](https://doi.org/10.1016/S0165-6147(00)01643-6).
- [91]. Trang, T., Beggs, S., Salter, M.W., (2012). ATP receptors gate microglia signaling in neuropathic pain. *Exp. Neurol.* **234**, 354–361. <https://doi.org/10.1016/j.expneurol.2011.11.012>.
- [92]. Burnstock, G., (2008). Purinergic signalling and disorders of the central nervous system. *Nature Rev. Drug Discov.* **7**, 575–590. <https://doi.org/10.1038/nrd2605>.
- [93]. Cheffer, A., Castillo, A.R.G., Corrêa-Velloso, J., Gonçalves, M.C.B., Naaldijk, Y., Nascimento, I.C., et al., (2018). Purinergic system in psychiatric diseases. *Mol. Psychiatry* **23**, 94–106. <https://doi.org/10.1038/mp.2017.188>.
- [94]. Berne, R.M., (1980). The role of adenosine in the regulation of coronary blood flow. *Circ. Res.* **47**, 807–813. <https://doi.org/10.1161/01.RES.47.6.807>.
- [95]. Dunwiddie, T.V., Masino, S.A., (2001). The role and regulation of adenosine in the central nervous system. *Annu. Rev. Neurosci.* **24**, 31–55. <https://doi.org/10.1146/annurev.neuro.24.1.31>.
- [96]. Haskó, G., Cronstein, B.N., (2004). Adenosine: an endogenous regulator of innate immunity. *Trends Immunol.* **25**, 33–39. <https://doi.org/10.1016/j.it.2003.11.003>.
- [97]. Wilson, R.I., Nicoll, R.A., (2002). Endocannabinoid signaling in the brain. *Science* **296**, 678–682. <https://doi.org/10.1126/science.1063545>.
- [98]. Castillo, P.E., Younts, T.J., Chávez, A.E., Hashimoto, Y., (2012). Endocannabinoid signaling and synaptic function. *Neuron* **76**, 70–81. <https://doi.org/10.1016/j.neuron.2012.09.020>.
- [99]. Mechoulam, R., Parker, L.A., (2013). The endocannabinoid system and the brain. *Annu. Rev. Psychol.* **64**, 21–47. <https://doi.org/10.1146/annurev-psych-113011-143739>.
- [100]. Harris, S.G., Padilla, J., Koumas, L., Ray, D., Phipps, R. P., (2002). Prostaglandins as modulators of immunity. *Trends Immunol.* **23**, 144–150. [https://doi.org/10.1016/S1471-4906\(01\)02154-8](https://doi.org/10.1016/S1471-4906(01)02154-8).
- [101]. Huang, Z.-L., Urade, Y., Hayaishi, O., (2007). Prostaglandins and adenosine in the regulation of sleep and wakefulness. *Curr. Opin. Pharmacol.* **7**, 33–38. <https://doi.org/10.1016/j.coph.2006.09.004>.
- [102]. Saper, C.B., Romanovsky, A.A., Scammell, T.E., (2012). Neural circuitry engaged by prostaglandins during the sickness syndrome. *Nature Neurosci.* **15**, 1088–1095. <https://doi.org/10.1038/nn.3159>.
- [103]. Hökfelt, T., Johansson, O., Ljungdahl, Å., Lundberg, J. M., Schultzberg, M., (1980). Peptidergic neurones. *Nature* **284**, 515–521. <https://doi.org/10.1038/284515a0>.
- [104]. Hökfelt, T., Broberger, C., Xu, Z.-Q.-D., Sergeev, V., Ubink, R., Diez, M., (2000). Neuropeptides – an overview. *Neuropharmacology* **39**, 1337–1356. [https://doi.org/10.1016/S0028-3908\(00\)00010-1](https://doi.org/10.1016/S0028-3908(00)00010-1).
- [105]. Saper, C.B., Scammell, T.E., Lu, J., (2005). Hypothalamic regulation of sleep and circadian rhythms. *Nature* **437**, 1257–1263. <https://doi.org/10.1038/nature04284>.
- [106]. Arora, S., Anubhuti, (2006). Role of neuropeptides in appetite regulation and obesity – a review. *Neuropeptides* **40**, 375–401. <https://doi.org/10.1016/j.npep.2006.07.001>.
- [107]. Vosko, A.M., Schroeder, A., Loh, D.H., Colwell, C.S., (2007). Vasoactive intestinal peptide and the mammalian circadian system. *Gen. Comp. Endocrinol.* **152**, 165–175. <https://doi.org/10.1016/j.ygcen.2007.04.018>.
- [108]. Meyer-Lindenberg, A., Domes, G., Kirsch, P., Heinrichs, M., (2011). Oxytocin and vasopressin in the human brain: social neuropeptides for translational medicine. *Nature Rev. Neurosci.* **12**, 524–538. <https://doi.org/10.1038/nrn3044>.
- [109]. Fields, H., (2004). State-dependent opioid control of pain. *Nature Rev. Neurosci.* **5**, 565–575. <https://doi.org/10.1038/nrn1431>.
- [110]. Le Merrer, J., Becker, J.A.J., Befort, K., Kieffer, B.L., (2009). Reward processing by the opioid system in the brain. *Physiol. Rev.* **89**, 1379–1412. <https://doi.org/10.1152/physrev.00005.2009>.
- [111]. Al-Hasani, R., Bruchas, M.R., (2011). Molecular mechanisms of opioid receptor-dependent signaling and behavior. *Anesthesiology* **115**, 1363. <https://doi.org/10.1097/ALN.0b013e318238bba6>.
- [112]. Mogil, J.S., Pasternak, G.W., (2001). The molecular and behavioral pharmacology of the orphanin FQ/nociceptin peptide and receptor family. *Pharmacol. Rev.* **53**, 381–415. [https://doi.org/10.1016/S0031-6997\(24\)01502-3](https://doi.org/10.1016/S0031-6997(24)01502-3).

- [113]. Lambert, D.G., (2008). The nociceptin/orphanin FQ receptor: a target with broad therapeutic potential. *Nature Rev. Drug Discov.* **7**, 694–710. <https://doi.org/10.1038/nrd2572>.
- [114]. Lovinger, D.M., Mateo, Y., Johnson, K.A., Engi, S.A., Antonazzo, M., Cheer, J.F., (2022). Local modulation by presynaptic receptors controls neuronal communication and behaviour. *Nature Rev. Neurosci.* **23**, 191–203. <https://doi.org/10.1038/s41583-022-00561-0>.